Advances in Radiation Oncology (2021) 7, 100847

advances in radiation oncology

www.advancesradonc.org

Research Letter

Sequential Diffusion Tensor Imaging and Magnetic Resonance Spectroscopy in Patients Undergoing Reirradiation for Progressive Diffuse Intrinsic Pontine Glioma

Julianna K. Bronk, MD, PhD,[a] Ping Hou, PhD,[b] Mark J. Amsbaugh, MD,[a] Soumen Khatua, MD,[c] Anita Mahajan, MD,[d] Leena Ketonen, MD,[e] and Susan L. McGovern, MD, PhD[a,*]

[a]Departments of Radiation Oncology, The University of Texas MD Anderson Cancer Center, Houston, Texas; [b]Departments of Imaging Physics, The University of Texas MD Anderson Cancer Center, Houston, Texas; [c]Departments of Pediatrics, The University of Texas MD Anderson Cancer Center, Houston, Texas; [d]Department of Radiation Oncology, Mayo Clinic, Rochester, Minnesota; [e]Departments of Diagnostic Radiology, The University of Texas MD Anderson Cancer Center, Houston, Texas

Received December 7, 2020; accepted October 31, 2021

Abstract

Purpose: Diffusion tensor imaging for evaluation of white matter tracts is used with magnetic resonance spectroscopy (MRS) to improve management of diffuse intrinsic pontine glioma (DIPG). Changes in the apparent diffusion coefficient (ADC), fractional anisotropy (FA), and tumor metabolite ratios have been reported after initial radiation for DIPG, but these markers have not been studied sequentially in patients undergoing reirradiation for progressive DIPG. Here, we report a case series of 4 patients who received reirradiation for progressive DIPG on a prospective clinical trial in which we evaluated quantitative changes in FA, ADC, and tumor metabolites and qualitative changes in white matter tracts.

Methods and Materials: The median reirradiation dose was 25.2 Gy (24-30.8 Gy). Fiber tracking was performed using standard tractography analysis. The FA and ADC values for the corticospinal and medial lemniscus tracts were calculated before and after reirradiation. Multivoxel MRS was performed. Findings were correlated with clinical features and conventional MRI of tumors.

Results: All patients had an initial response to reirradiation as shown by a decrease in tumor size. In general, FA increased with disease response and decreased with progression, whereas ADC decreased with disease response and increased with progression. At second progression, the FA fold change relative to values during disease response decreased in both patients with available imaging at second progression. Visualization of tracts demonstrated robust reconstitution of previously disrupted paths during tumor response; conversely, there was increased fiber tract disruption and infiltration during tumor progression. The MRS analysis revealed a decrease in choline:creatinine and choline:N-acetylaspartate ratios during tumor response and increase during progression.

Conclusions: Distinct changes in white matter tracts and tumor metabolism were observed in patients with DIPG undergoing reirradiation on a prospective clinical trial. Changes related to tumor response and progression were observed after 24 to 30.8 Gy reirradiation.

Sources of support: This work had no specific funding.

Disclosures: none.

Research data are stored in an institutional repository and will be shared upon request to the corresponding author.

Clinical Trial: NCT01469247—Diffuse Intrinsic Pontine Glioma (DIPG) Reirradiation (ReRT)

*Corresponding author: Susan L. McGovern, MD, PhD; E-mail: slmcgove@mdanderson.org

https://doi.org/10.1016/j.adro.2021.100847

Introduction

Diffuse intrinsic pontine glioma (DIPG) is a uniformly fatal tumor mainly occurring in young children. Currently, radiation is the only effective therapy; however, disease progression eventually occurs in all patients. Difficulties in defining true tumor progression owing to significant variability in radiographic 2-dimensional tumor measurements using conventional magnetic resonance imaging (MRI) are confounded by challenges in delineating treatment-related changes from progressive disease.[1–4] Advanced brain tumor imaging techniques including diffusion tensor imaging (DTI) and magnetic resonance spectroscopy (MRS) allow for more precise assessment of upfront treatment response but have not been prospectively studied in patients undergoing reirradiation for progressive DIPG.[5–8]

We evaluated quantitative alterations in the apparent diffusion coefficient (ADC), fractional anisotropy (FA), and tumor metabolites in addition to qualitative changes in white matter tracts in a case series of 4 patients with progressive DIPG who underwent reirradiation on a prospective trial. Diffusion tensor imaging and MRS were performed before and serially after reirradiation. Tractography and spectroscopy results were correlated with clinical features of disease response and progression.

Methods

Patient data collection

All work was performed on an institutional review board–approved protocol at a single institution. The study population included 4 patients with progressive DIPG treated with reirradiation on a prospective trial.[9] Patient characteristics are summarized in Table 1. Reirradiation was initiated at least 10 months after completion of initial therapy. All patients underwent DTI before and after reirradiation at approximately 30-day intervals. Two patients had additional DTI scans after the second progression. Magnetic resonance spectroscopy was performed in 1 patient before reirradiation. All patients had MRS performed after reirradiation and 2 patients had MRS at second progression.

Imaging technique and tractography analysis

Diffusion tensor imaging and MRS of the brain were performed on a General Electric 3.0T system with 8-channel brain coil. The studies used 2-dimensional (2D) T2-weighted FLAIR images in the axial plane using 5-mm slice thickness with 0-mm interslice gap according to our routine pediatric brain protocol that is obtained with a field-of-view (FOV) of 20 cm and a 256 × 192 matrix. Response assessment in neuro-oncology (RANO) criteria were used as an objective tool for imaging assessment of treatment response.[10] As per the RANO criteria, 2D tumor measurements acquired at the maximum dimension of the lesion were used. T2-weighted FLAIR has become the standard neuroimaging technique used to assess treatment response because it is a sequence that best shows the nonenhancing component of the tumor such as that often seen in patients with DIPG.

The DTI was acquired in a FOV of 22 cm, 128 × 128 matrix, b-value of 1000 s/mm^2 with 27 diffusion directions and a slice thickness of 3.5 mm, to cover 120 to 150 mm of the brain and resulting in a scan time of 4 to 5 minutes. The DTI images were processed offline on a workstation after 2D geometric distortion correction. The direction of the maximum diffusivity was mapped by using red (left-right), green (anterior-posterior), and blue (superior-inferior) for each voxel, with color brightness modulated by the FA value. Regions of interest were manually delineated on the DTI color map at the level of the pons (Fig 1A).

Diffusion tensor imaging fiber tracking was generated from a seed point in both forward and backward directions defined by the major eigenvector at the seed point. The propagation was terminated when the trajectory reached a voxel with an FA less than 0.2 or when the angle between 2 consecutive steps was greater than 45°. The corticospinal tracts and medial lemniscus tracts were generated from the FA color maps following the same trajectory rule. The FA and ADC maps were generated from tensor eigenvalues and mean diffusivity, respectively,

$$FA = \sqrt{\frac{3}{2}}\sqrt{\frac{\left(\lambda_1 - \overline{\lambda}\right)^2 + \left(\lambda_2 - \overline{\lambda}\right)^2 + \left(\lambda_3 - \overline{\lambda}\right)^2}{\lambda_1{}^2 + \lambda_2{}^2 + \lambda_3{}^2}}$$

$$ADC = \frac{\lambda_1 + \lambda_2 + \lambda_3}{3}$$

where λ_1, λ_2, and λ_3 are the diffusion eigen values in 3 orthogonal directions and $\overline{\lambda}$ is the mean of all the eigen values.

Multivoxel MRS analysis

Two-dimensional multivoxel Point RESolved Spectroscopy chemical shift imaging was acquired with a repetition time/echo time of 1000/144 msec, 16 × 16 frequency and phase, number of excitations of 2, and 15-mm slice thickness. Routine MRS preprocessing, such as water subtraction and phase correction, was applied before 3-

Table 1 Patient characteristics and clinical course

Patient number	Age at re-RT, y	Sex	Initial dose, Gy	Initial fractions, No.	Time from first RT to re-RT, mo	Re-RT dose, Gy	Re-RT fractions, No.	Time from re-RT to death, mo	Symptoms before re-RT	Symptoms after re-RT	Symptoms at second progression
1	5	Male	54	30	10	30.8	14	6	Lethargy, weakness, swallowing dysfunction requiring nasogastric tube feeding	Ambulation improved, improved left upper extremity weakness	NA
2	6	Female	54	30	10	24	12	4	Left upper and lower extremity weakness, gait imbalance	Significant improvement in lower extremity strength, left arm mobility, and ability to walk	Increase in left upper and lower extremity weakness; required assistance with walking, broad-based gait
3	4	Male	54	30	15	24	12	5	Left upper extremity weakness, slurred and slow speech; slow, broad-based gait with ataxia	Improvement in speech, steadier gait	Worsened speech and gait; new difficulty swallowing and with eye movements; weakness and rigidity in right hand and foot; dysmetria of the left upper extremity with weakness
4	26	Female	54	30	72	26.4	12	21	Diplopia, ataxia, dysphagia, slurred speech; decreased sensation and movement of right face	Improvement in vision, gait, speech, swallow, and voice; stable numbness and weakness of right face	NA

Abbreviations: Gy = Gray; NA = not applicable; re-RT = reirradiation.

dimensional (2 dimensions for space and 1 for time) Fourier transformation of the MRS data from time domain to frequency domain. After baseline correction and Levenberg-Marquardt curve fitting in the frequency domain, metabolites choline (Cho), N-acetylaspartate (NAA), creatinine (Cr), and lipid lactate were analyzed in the desired frequency region. The sum value (area under the curve) and the ratio were reported in the spectrum. The final spectrum was overlaid on the anatomic image, and the spectrum value and plot for each region of interest were saved.

Fold change calculations

The fold change of quantitative variables at response and progression was calculated as follows:

Fold change (progression to response):

$$D_{fold\ change} = \frac{\overline{D}_{response} - \overline{D}_{progression}}{\overline{D}_{progression}}$$

Fold change (response to progression):

$$D_{fold\ change} = \frac{\overline{D}_{progression} - \overline{D}_{response}}{\overline{D}_{response}}$$

where $\overline{D}$ is the average value (FA, ADC, Cho:Cr, or Cho:NAA) for patients with values at multiple time points.

Case series

All patients had an initial response to reirradiation as shown by a decrease in tumor size (Table 2). Furthermore, all patients had improvement in clinical symptoms after reirradiation and worsening of symptoms or development of new deficits on second progression (Table 1).

Case 1: Qualitative and quantitative changes in DTI and MRS before and after reirradiation corresponded with patient neurologic status

A 5-year-old boy underwent reirradiation for recurrent DIPG to a dose of 30.8 Gy in 14 fractions 10 months after initial treatment. Before reirradiation, he had symptoms of lethargy, weakness, and swallowing dysfunction requiring nasogastric tube feeding. After reirradiation, the patient had improvements in ambulation and left upper extremity weakness and no longer was dependent on tube feeds. The DTI color FA maps before and after reirradiation showed improvement in integrity and visualization of tract fibers 24 days after reirradiation (Fig 1A,B). An increase in FA (from 0.337 before reirradiation to 0.474 after reirradiation; fold change, 0.41) and a decrease in ADC (from 1.35×10^{-9} m^2/s to 1.03×10^{-9} m^2/s after reirradiation; fold change, −0.24) correlated with tumor response shown by a decrease in cross-sectional tumor area from 1409 cm^2 to 1149 cm^2 (Table 2 and Fig 1C). Likewise, MRS analysis performed at first progression before undergoing reirradiation revealed elevation in metabolite ratios (Cho:Cr, 2.8, and Cho:NAA, 1.7), which subsequently decreased during disease response (1.8 and 1.4, respectively; fold change, −0.36 and −0.18, respectively) (Table 3). Because

quantitative DTI and MRS analyses were consistent with disease response as well as improvement in DTI tractography with corresponding improvement in neurologic status, a new patchy area of enhancement along the left ventral aspect of the pons visualized on the postcontrast T1 sequence was thought to be consistent with treatment effect (Fig 1D).

Cases 2 and 3: Qualitative and quantitative changes in sequential DTI and MRS after reirradiation corresponded to tumor response to reirradiation and second progression

Patients 2 and 3 had sequential DTI scans at first progression, at response to reirradiation, and at second progression. The patients, a 6-year-old female and a 4-year-old male, were both treated to a dose of 24 Gy in 12 fractions for disease progression 10 and 15 months after initial radiation treatment, respectively. Tractography of the medial lemniscus tracts demonstrated robust reconstitution of previously disrupted paths during the initial tumor response to reirradiation for both patients (Fig 2A,B). The fold change in FA during response when normalized to prereirradiation values was −0.05 in patient 2 and 0.89 in patient 3. With second tumor progression, a decrease in FA was observed in both patients (the fold change when normalized to values during response was −0.48 and −0.36, respectively). The fold change in ADC during response when normalized to prereirradiation values was 0.32 in patient 2 and −0.27 in patient 3. With the second tumor progression, an increase in ADC was observed in both patients (the fold change when normalized to values during response was 0.48 and 0.04, respectively; Table 2). An example of multivoxel MRS analysis performed after reirradiation and at second progression is shown in Figure 2C,D. On MRS analysis, the Cho:Cr ratio increased with second disease progression (the fold change was 0.37 for patient 2 and 1.00 for patient 3). The Cho:NAA ratio did not consistently change with tumor progression (Table 3).

Case 4: With sustained response to reirradiation, analysis of sequential DTI and MRS reflected stable treated disease

A 26-year-old woman underwent reirradiation for recurrent DIPG to a dose of 26.4 Gy in 12 fractions 21 months after initial treatment and had a sustained response with DTI tractography demonstrating clear connection of the medial lemniscus and corticospinal tract fibers up to 308 days after treatment completion (Fig 3A, B). An increase in FA (fold change of 0.14) and a decrease in ADC (fold change of −0.22) correlated with tumor response (Table 2). On the first follow-up after reirradiation, there was new enhancement noted along the anterior and anterolateral aspects of the pons with corresponding increase in FLAIR signal. Enhancement decreased and resolved on subsequent follow-up MRI scans and was accompanied by improvement of tumor appearance on T2 FLAIR sequences (Fig 3C,D). Tissue metabolites remained stable on MRS analysis (Table 3). This patient died from unknown causes 21 months after completing reirradiation.

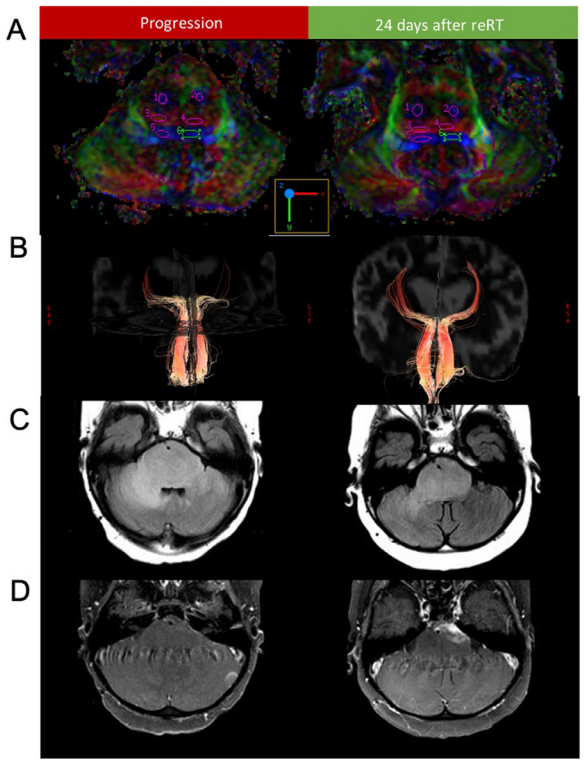

Fig. 1 (A) Diffusion tensor imaging color fractional anisotropy maps and region of interest delineation of the corticospinal (1,2), transverse pontine (3,4), and medial lemniscus (5,6) fibers before and after reirradiation are shown for patient 1. (B) Diffusion tensor imaging tractography of the medical lemniscus tracts before and after reirradiation. T2-FLAIR (C) and T1-post-contrast (D) sequences are shown before reirradiation and after reirradiation.

Discussion

Brain stem gliomas infiltrate the white matter network in the brain stem, leading to bulk displacement, disruption of organization, or complete destruction of long tracts mediated by tumor growth. Prabhu et al reported

Table 2 Tumor size and quantitative DTI analysis

Patient number	Time from re-RT, mo	Tumor cross-sectional area, cm^2	FA	FA foldchange	ADC $\times 10^{-9}$ m^2/s	ADC fold change	Outcome
1	0.0	1409	0.337	Fold change (progression to response)	1.35	Fold change (progression to response)	Progression
	0.8	1149	0.474	0.41	1.03	−0.24	Response
2	0.0	1534	0.239	Fold change (progression to response)	0.88	Fold change (progression to response)	Progression
	1.1	1308	0.210	−0.05	1.40	0.32	Response
	2.3	1319	0.244	Fold change (response to progression)	0.92	Fold change (response to progression)	Response
	3.4	1438	0.118	−0.48	1.71	0.48	Progression
3	0.0	1495	0.158	Fold change (progression to response)	1.36	Fold change (progression to response)	Progression
	1.1	1372	0.298	0.89	0.99	−0.27	Response
	2.2	1625	0.193	Fold change (response to progression)	0.99	Fold change (response to progression)	Progression
	4.3	1826	0.189	−0.36	1.07	0.04	Progression
4	0.0	1759	0.487		1.24		Progression
	1.1	1583	0.589		0.98		Response
	4.4	1555	0.541		0.92		Response
	6.0	1415	0.500	Fold change (progression to response)	1.06	Fold change (progression to response)	Response
	10.3	1266	0.600	0.14	0.91	−0.22	Response

Abbreviations: ADC = apparent diffusion coefficient; DTI = diffusion tensor imaging; FA = fractional anisotropy; re-RT = reirradiation.

Table 3 Magnetic resonance spectroscopy analysis and enhancement

Patient number	Time from re-RT, mo	Lipid peak	Cho:Cr	Fold change	Cho:NAA	Fold change	Enhancement	Outcome
1	0.0	Yes	2.8	Fold change (progression to response)	1.7	Fold change (progression to response)	None	Progression
	0.8	Yes, tall	1.8	−0.36	1.4	−0.18	New	Response
2	1.1	Yes	2.1		2.4		Stable	Response
	2.3	Yes	3.6	Fold change (response to progression)	4.6	Fold change (response to progression)	Stable	Response
	3.4	No	3.9	0.37	2.8	−0.20	Progressive	Progression
3	1.1	No	1.7		1.1		Progressive	Response
	2.2	Yes	3.6	Fold change (response to progression)	1.6	Fold change (response to progression)	Progressive	Progression
	4.3	No	3.2	1.00	2.1	0.68	Progressive	Progression
4	1.1	Yes	2.5		1.2		New	Response
	4.4	No	4.1		1.2		Decreased	Response
	10.3	Yes	2.5		1.6		None	Response

Abbreviations: Cho = choline; Cr = creatinine; NAA = N-acetylaspartate; re-RT = reirradiation.

on DTI assessment in 3 patients newly diagnosed with DIPG treated with combination chemotherapy and radiation therapy.[11] Disruption of fiber tracts was noted with disease progression. An age-matched ADC ratio compared with normal controls was calculated, and the authors found a decrease in ADC tumor values after initial treatment and an increase in ADC during progression. Likewise, in a retrospective study, Khatua et al[12] reported changes in FA values after a single time point after reirradiation to 20 Gy in 10 fractions in 6 patients. An increase in FA was noted during treatment response, which also correlated with clinical improvement.

In our series of 4 patients with progressive DIPG treated with reirradiation and followed prospectively with DTI, all had an initial response to reirradiation as shown by a decrease in tumor size and in qualitative improvement in 3-dimensional tractography. Clinically, these patients improved after reirradiation with improvement in motor function, vision, and speech. All but 1 patient displayed an increase in FA and a decrease in ADC during response to reirradiation. All patients with imaging at second progression had a decrease in FA and a small increase in ADC. Our findings correlate with trends previously reported in the literature discussed above, although FA and ADC have not been examined in combination in the same patient cohort, and data were not collected prospectively as was done in this study.

Characterization of MR spectra can be applied toward tumor grading, prediction of tumor response to the treatment, selection of an active, invasive part of the tumor for

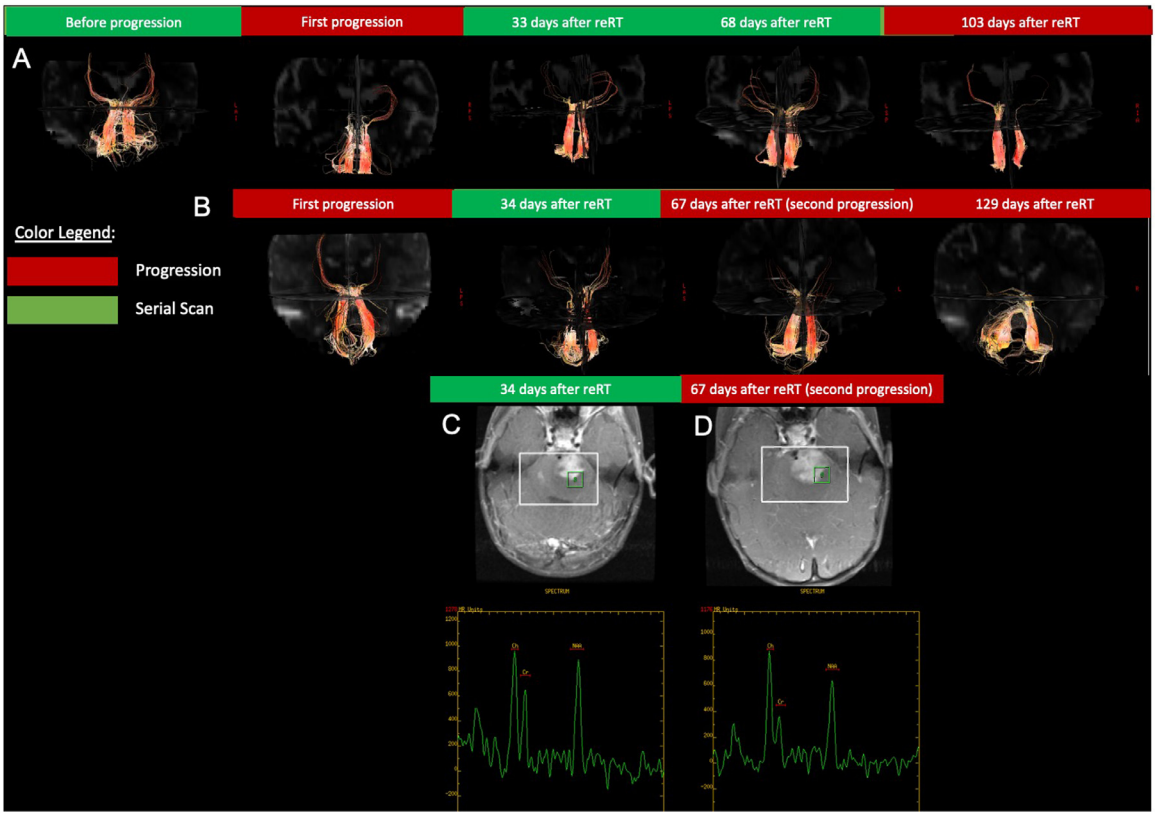

Fig. 2 Diffusion tensor imaging tractography of the medial lemniscus tracts in patient 2 (A) and patient 3 (B) are shown before reirradiation, during treatment response, and at second progression. Multivoxel magnetic resonance spectroscopy after re-irradiation (C) and at second progression (D) for patient 3. Decrease in metabolites including N-acetylaspartate (6562-4811) and creatinine (4095-2314) with progression is noted. Likewise, progression of enhancement on T1 postcontrast sequence corresponding to active disease is noted.

biopsy or surgical resection, and radiation treatment planning. Likewise, after treatment completion, MRS can be used to assess for tumor stability or progression.[13] We found detectable changes in tumor metabolites after reirradiation and at second progression. Spectroscopic changes after reirradiation were consistent with previously reported trends after initial radiation therapy for patients with DIPG with overall decrease in Cho:Cr and Cho:NAA ratios observed during tumor response and increase at tumor progression.[7] The Cho:Cr ratios were most consistent with disease progression and response in this series of patients. An increase in Cho:NAA at any time point has been shown to be prognostic of worse overall survival outcomes in DIPG.[8] In patient 4, with more than 300 days of response to reirradiation, a stable Cho:NAA ratio was observed during the posttreatment time points assessed.

Diffuse intrinsic pontine glioma is characteristically nonenhancing on postcontrast T1-weighted images, and development of overt contrast enhancement has been associated with poor outcomes.[14,15] All patients had new or progressive enhancement present at first imaging after reirradiation despite radiographic, metabolic, and tractography analysis suggesting disease response. Progressive enhancement was observed at the second progression.

A chief limitation of this study was the small number of patients, which restricts our ability to draw conclusions as to the utility of advanced imaging studies such as DTI and MRS when evaluating disease response in patients with DIPG undergoing reirradiation. However, on examination of the trends in our patient cohort, we found that the effects on FA fold change on second progression and Cho:Cr ratio during disease response were most consistent, suggesting a utility for these measurements with sequential DTI and MRS analyses. However, small inconsistencies in trends in other quantitative measurements including the ADC and the Cho:NAA ratio during disease response and progression do not necessarily rule out the utility of these metrics, which warrant further investigation in a larger patient group. An additional limitation that may contribute to inconsistencies in quantitative trends observed in this study include that we applied RANO criteria for sequential assessment of tumor size in this analysis, which was used to correlate

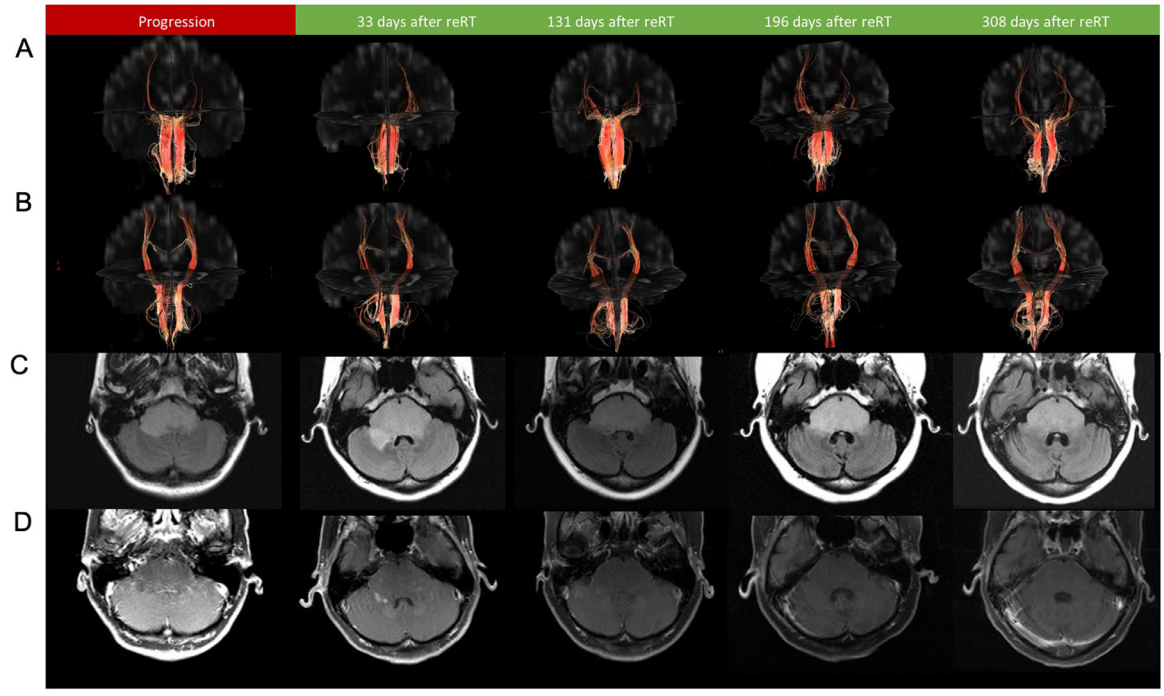

Fig. 3 Diffusion tensor imaging tractography of the medial lemniscus (A) and corticospinal tracts (B) of patient 4 with sustained response up to 308 days after reirradiation. T2-FLAIR (C) and T1-postcontrast (D) sequences at the level of the pons are shown at each time point.
Abbreviations: ADC = apparent diffusion coefficient; Cho = choline; Cr = creatinine; DTI = diffusion tensor imaging; FA = fractional anisotropy; NAA = N- acetylaspartate.

DTI and MRS measurements with disease response. Although the primary focus of the RANO effort was to improve the conduct of clinical trials, it is useful in the routine care of patients with brain tumors, especially those with nonenhancing lesions. Whereas RANO has become the mainstay of assessment in tumor treatment response because it is fast and can be reliably duplicated and performed during primary reading without requiring assessment on different workstations, evolving volumetric imaging techniques such as 3D-FLAIR and postcontrast T1-weighted images, as well as advanced physiological imaging techniques such as MRS, arterial spin labeling, and dynamic contrast enhanced and dynamic susceptibility contrast MRI, have potential to be adapted into standardized response metrics and may be considered as part of the standard pediatric brain protocol in the future.[16–18] To evaluate the utility of these modalities, future investigational studies should be designed to examine not only functional imaging—specific information in relation to RANO criteria but also clinical outcomes including symptom relief and overall survival.

In conclusion, we found that reconstitution of white matter tracts correlated with clinical observations of improvement in patient symptoms during disease response. Quantitative changes in FA, ADC, and tumor metabolites during treatment response to reirradiation and at second progression were consistent with previously reported trends described in an initial radiation setting. Although investigation of novel strategies to treat progressive DIPG are ongoing, these data support further prospective investigation of advanced imaging techniques including DTI and MRS during assessment of disease response.

Supplementary materials

Supplementary material associated with this article can be found in the online version at doi:10.1016/j.adro.2021.100847.

References

1. Barkovich AJ, Krischer J, Kun LF, et al. Brain stem gliomas: A classification system based on magnetic resonance imaging. *Pediatr Neurosurg*. 1990;16:73–83.
2. Fischbein NJ, Prados MD, Wara W, Russo C, Edwards MS, Barkovich AJ. Radiologic classification of brain stem tumors: Correlation of magnetic resonance imaging appearance with clinical outcome. *Pediatr Neurosurg*. 1996;24:9–23.

3. Liu AK, Brandon J, Foreman NK, Fenton LZ. Conventional MRI at presentation does not predict clinical response to radiation therapy in children with diffuse pontine glioma. *Pediatr Radiol*. 2009;39:1317–1320.
4. Hayward RM, Patronas N, Baker EH, Vezina G, Albert PS, Warren KE. Inter-observer variability in the measurement of diffuse intrinsic pontine gliomas. *J Neurooncol*. 2008;90:57–61.
5. Tisnado J, Young R, Peck KK, Haque S. Conventional and advanced imaging of diffuse intrinsic pontine glioma. *J Child Neurol*. 2016;31:1386–1393.
6. Panigrahy A, Nelson Jr. MD, Finlay JL, et al. Metabolism of diffuse intrinsic brainstem gliomas in children. *Neuro Oncol*. 2008;10:32–44.
7. Laprie A, Pirzkall A, Haas-Kogan DA, et al. Longitudinal multivoxel MR spectroscopy study of pediatric diffuse brainstem gliomas treated with radiotherapy. *Int J Radiat Oncol Biol Phys*. 2005;62:20–31.
8. Steffen-Smith EA, Shih JH, Hipp SJ, Bent R, Warren KE. Proton magnetic resonance spectroscopy predicts survival in children with diffuse intrinsic pontine glioma. *J Neurooncol*. 2011;105:365–373.
9. Amsbaugh MJ, Mahajan A, Thall PF, et al. A phase 1/2 trial of reirradiation for diffuse intrinsic pontine glioma. *Int J Radiat Oncol Biol Phys*. 2019;104:144–148.
10. Chukwueke UN, Wen PY. Use of the Response Assessment in Neuro-Oncology (RANO) criteria in clinical trials and clinical practice. *CNS Oncol*. 2019;8:CNS28.
11. Prabhu SP, Ng S, Vajapeyam S, Kieran MW, Pollack IF. DTI assessment of the brainstem white matter tracts in pediatric BSG before and after therapy: A report from the Pediatric Brain Tumor Consortium. *Childs Nerv Syst*. 2011;27:11–18.
12. Khatua S, Hou P, Bodiwala R, et al. Preliminary experience with diffusion tensor imaging before and after re-irradiation treatments in children with progressive diffuse pontine glioma. *Childs Nerv Syst*. 2014;30:925–930.
13. Faghihi R, Zeinali-Rafsanjani B, Mosleh-Shirazi MA, et al. magnetic resonance spectroscopy and its clinical applications: A review. *J Med Imaging Radiat Sci*. 2017;48:233–253.
14. Poussaint TY, Kocak M, Vajapeyam S, et al. MRI as a central component of clinical trials analysis in brainstem glioma: A report from the Pediatric Brain Tumor Consortium (PBTC). *Neuro Oncol*. 2011;13:417–427.
15. Jansen MH, Veldhuijzen van Zanten SE, Sanchez Aliaga E, et al. Survival prediction model of children with diffuse intrinsic pontine glioma based on clinical and radiological criteria. *Neuro-oncology*. 2015;17:160–166.
16. Alsop DC, Detre JA, Golay X, et al. Recommended implementation of arterial spin-labeled perfusion MRI for clinical applications: A consensus of the ISMRM perfusion study group and the European consortium for ASL in dementia. *Magn Reson Med*. 2015;73:102–116.
17. Sourbron SP, Buckley DL. On the scope and interpretation of the Tofts models for DCE-MRI. *Magn Reson Med*. 2011;66:735–745.
18. Shiroishi MS, Castellazzi G, Boxerman JL, et al. Principles of T2*-weighted dynamic susceptibility contrast MRI technique in brain tumor imaging. *J Magn Reson Imaging*. 2015;41:296–313.